

## **Custom long non-coding RNA capture enhances detection sensitivity in different human sample types**

Annelien Morlion<sup>1,2\*</sup>, Celine Everaert<sup>1,2\*</sup>, Justine Nuytens<sup>1,2</sup>, Eva Hulstaert<sup>1,2,3</sup>, Jo Vandesompele<sup>1,2</sup>, Pieter Mestdagh<sup>1,2°</sup>

<sup>1</sup> OncoRNALab, Center for Medical Genetics, Department of Biomolecular Medicine, Ghent University, Ghent, Belgium

<sup>2</sup> Cancer Research Institute Ghent (CRIG), Ghent, Belgium

<sup>3</sup> Department of Dermatology, Ghent University Hospital, Ghent, Belgium

\*joint first authors

°corresponding author: [pieter.mestdagh@ugent.be](mailto:pieter.mestdagh@ugent.be)

## 1 Abstract

2 Long non-coding RNAs (lncRNAs) are a heterogeneous group of transcripts that lack protein  
3 coding potential and display regulatory functions in various cellular processes. As a result of  
4 their cell- and cancer-specific expression patterns, lncRNAs have emerged as potential  
5 diagnostic and therapeutic targets. The accurate characterization of lncRNAs in bulk  
6 transcriptome data remains challenging due to their low abundance compared to protein  
7 coding genes. To tackle this issue, we describe a unique short-read custom lncRNA capture  
8 sequencing approach that relies on a comprehensive set of 565,878 capture probes for 49,372  
9 human lncRNA genes. This custom lncRNA capture approach was evaluated on various sample  
10 types ranging from artificial high-quality RNA mixtures to more challenging formalin-  
11 fixed paraffin-embedded tissue and biofluid material. The custom enrichment approach  
12 allows the detection of a more diverse repertoire of lncRNAs, with better reproducibility and  
13 higher coverage compared to classic total RNA-sequencing.

14

## 15 Keywords

16 lncRNA, RNA sequencing, probes, lncRNome, RNA abundance, RNA expression, FFPE, biofluid

17

## 18 Introduction

19 While the majority of the human genome is actively transcribed into RNA transcripts, most of  
20 these transcripts do not code for proteins (Djebali *et al.*, 2012). The non-coding RNA  
21 transcripts longer than 200 nucleotides belong to the heterogeneous group of long non-  
22 coding RNAs (lncRNAs), half of which are not poly-adenylated (Lorenzi *et al.*, 2019). These  
23 lncRNAs are known to influence gene expression at both the transcriptional and post-  
24 transcriptional level through a variety of mechanisms (Mercer *et al.*, 2009; Robinson *et al.*,  
25 2020). Moreover, lncRNAs often show a particular cell- or cancer-type specific expression  
26 pattern (Iyer *et al.*, 2015), which adds to their biomarker potential.

27 In the past, several high-throughput methods have been developed to profile the long non-  
28 coding RNA transcriptome, study their structure or define their function (Cao *et al.*, 2019;  
29 Turner *et al.*, 2019). Because of their generally low abundance compared to protein coding  
30 genes, quantification of lncRNAs in bulk transcriptome data remains challenging. Enrichment  
31 strategies favoring lncRNAs over the more abundant mRNAs could therefore result in more

32 lncRNAs being detected with a better transcript coverage, improving downstream analysis. A  
33 promising method is RNA capture sequencing, a short-read sequencing method that can  
34 enrich RNA targets of interest using oligonucleotide probes that are specifically designed to  
35 tile the target sequences. These RNA capture sequencing technologies have mainly been  
36 applied for deep sequencing of a selection of lncRNAs (Mercer *et al.*, 2014; Clark *et al.*, 2015).  
37 Recently, the GENCODE consortium extended this method by applying long-read sequencing  
38 after capturing about 14,470 lncRNAs genes to improve their structural annotation (RNA  
39 Capture Long Seq, RNA CLS) (Lagarde *et al.*, 2017).

40 In this study, we describe a custom lncRNA capture sequencing approach that targets a very  
41 comprehensive human lncRNome. This custom capture approach was evaluated on various  
42 sample types ranging from high-quality RNA mixtures to more challenging formalin-  
43 fixed paraffin-embedded (FFPE) tissue and biofluid material.

44

## 45 Material and methods

### 46 *Probe design*

47 Probes were designed against the highly confident set of LNCipedia 5.2 (hg19 genome build).  
48 First, extended exons were created by concatenating each set of overlapping exons. For each  
49 of these extended exons, probes of 120 nucleotides were tiled, resulting in (number of  
50 nucleotides)-119 probes per concatenated exon. These exon tiling probes were mapped  
51 against repeat regions and protein coding genes to filter out these that would capture off-  
52 target fragments.

53 The resulting probe pool was extended with probes designed to capture both the Sequin and  
54 ERCC spikes. These probes are 120-mers designed by tiling the spike-in sequences and,  
55 inherent to the spike-design, these do not align to the human genome.

56 Further filtering was done by retaining the 120-mers with a GC content between 25-70%, a  
57 GC-based  $T_m$  between 60-80 °C and a  $\Delta G$  larger than -7 (calculated by UNAFold (version 3.8)  
58 settings: hybrid-ss-min -E -n DNA -t 54 -T 54). The remaining probes underwent a selection  
59 aimed at obtaining the minimal number of probes for an optimal coverage. In total, 565,878  
60 probes against LNCipedia, 81,089 probes against novel genes (not discussed in this paper) and  
61 2427 spike-in RNA probes were retained. Probes were synthesized by Twist Biosciences.

62

63 *Sample collection and RNA purification*

64 Sample collection was approved by the ethics committee of Ghent University Hospital, Ghent,  
65 Belgium (#B670201734450 and #B670201733701) and written informed consent was  
66 obtained from all donors. FFPE tissues were obtained from two colon cancer patients; the  
67 biofluid samples (seminal and blood plasma) were collected from healthy donors.

68 *Platelet depleted blood plasma*

69 Venous blood from two healthy donors was drawn from an elbow vein after disinfection with  
70 2% chlorhexidine in 70% alcohol. All blood draws were performed with a butterfly needle of  
71 21 gauge (BD Vacutainer, Push Button Blood Collection Set, #367326, Becton Dickinson and  
72 Company, NJ, USA) and blood was collected in 10 ml BD Vacutainer K2-EDTA tubes (#367525,  
73 Becton Dickinson and Company, NJ, USA). The tubes were inverted 5 times and centrifuged  
74 immediately after blood draw (15 min at 2500 g, room temperature, without brake). Per  
75 donor, the upper plasma fractions were pipetted (leaving approximately 0.5 cm plasma above  
76 the buffy coat) and pooled in a 15 ml tube. After gently inverting, the pooled plasma fraction  
77 was centrifuged again (15 min at 2500 g, room temperature, without brake) and the upper  
78 fraction was transferred to a new 15 ml tube, leaving approximately 0.5 cm plasma above  
79 the separation. The resulting platelet depleted plasma was gently inverted, snap-frozen in  
80 five aliquots (Safe-Lock cup DNA LoBind 2 ml PCR clean tubes, Eppendorf, #0030108078) and  
81 stored at -80 °C. Platelets were counted and the degree of hemolysis was determined by  
82 measuring levels of free hemoglobin by spectral analysis using a NanoDrop 1000  
83 Spectrophotometer (Thermo Fisher Scientific). The entire plasma preparation protocol was  
84 finished in two and a half hours. 200 µl was used for each RNA isolation.

85 *Seminal plasma*

86 Semen samples of healthy donors were produced by masturbation into a sterile container  
87 and were allowed to liquefy for 30 min at 37 °C. Samples were centrifuged to remove  
88 contaminating cells (10 min at 2000 g, room temperature, without brake) and stored at -80  
89 °C within two hours after collection. 200 µl was used for each RNA isolation.

90 *Biofluid RNA purification*

91 RNA was isolated with the miRNeasy Serum/Plasma Kit (Qiagen, #217184) according to the  
92 manufacturer's instructions. An input volume of 200 µL was used for all samples. Per 200 µL  
93 biofluid input volume, 2 µL sequin spike-in controls (Garvan Institute of Medical Research)  
94 were added before RNA isolation, in a 1/1300 000 dilution to blood plasma and in 1/1300

95 dilution to seminal plasma. Total RNA was eluted in 12  $\mu$ L of RNase-free water for (blood)  
96 platelet depleted plasma, and in 20  $\mu$ L of RNase-free water for seminal plasma – in order to  
97 adjust for viscosity. After RNA isolation, 2  $\mu$ L External RNA Control Consortium (ERCC) spike-  
98 in controls (ThermoFisher Scientific, #4456740) were added to the RNA isolation eluate of  
99 blood plasma and seminal plasma in a dilution of 1/1000 000 and 1/1000, respectively. gDNA  
100 heat-and-run removal was performed by adding 1  $\mu$ L HL-dsDNase (ArcticZymes #70800-202,  
101 2 U/ $\mu$ L) and 1.4  $\mu$ L reaction buffer (ArcticZymes #66001) to the combination of 12  $\mu$ L RNA  
102 eluate and 2  $\mu$ L ERCC spikes, followed by an incubation of 10 min at 37 °C and 5 min at 58 °C.  
103 RNA was stored at -80 °C and only thawed on ice immediately before the start of the library  
104 prep. Multiple freeze-thaw cycles did not occur. RNA obtained from three RNA isolations was  
105 pooled per biofluid and per sample to avoid RNA isolation induced variation. This pooled RNA  
106 was used as starting material for the different library preparations.

#### 107 *FFPE*

108 Tumor RNA was isolated from five 10  $\mu$ M sections of a formalin-fixed paraffin embedded  
109 (FFPE) tissue block, applying macrodissection based on histopathological evaluation of  
110 hematoxylin and eosin stained slides to select regions with high tumor cellularity. Within two  
111 days after sectioning, the tissue sections were scraped into microcentrifuge tubes,  
112 centrifuged for 5 min at 20,000 g, and deparaffinized in 320  $\mu$ L Deparaffinization Solution  
113 (Qiagen, #19093) for 3 min at 56 °C on a thermomixer (500 rpm). Samples were then cooled  
114 to room temperature for 15 min. Subsequently, RNA was isolated using the miRNeasy FFPE  
115 Kit (Qiagen, #217504), according to the manufacturer's protocol. gDNA heat-and-run removal  
116 was performed by adding 1  $\mu$ L HL-dsDNase (ArcticZymes #70800-202, 2 U/ $\mu$ L) and 0.68  $\mu$ L  
117 reaction buffer (ArcticZymes #66001) to 6.82  $\mu$ L RNA (100 ng), followed by an incubation of  
118 10 min at 37 °C and 5 min at 58 °C.

#### 119 *MAQCA/B*

120 Two commercially available RNA samples, MAQCA and MAQCB, were used. MAQCA is the  
121 Quantitative PCR Human Reference Total RNA (#750500, Agilent technologies), extracted  
122 from cell lines representing different human tissues. MAQCB is FirstChoice Human Brain  
123 Reference RNA (#AM7962, Life Technologies). gDNA heat-and-run removal was performed  
124 on both RNA samples by adding 1  $\mu$ L HL-dsDNase (ArcticZymes #70800-202, 2 U/ $\mu$ L) and 0.68  
125  $\mu$ L reaction buffer (ArcticZymes #66001) to 6.82  $\mu$ L RNA (100 ng), followed by an incubation of  
126 10 min at 37 °C and 5 min at 58 °C.

127 *Library preparation*

128 After RNA purification, four libraries were prepared for each sample: two technical replicates  
129 for total RNA-seq and two technical replicates for custom lncRNA capture sequencing.

130 *SMARTer Stranded Total RNA library preparation*

131 Sequencing libraries were generated using SMARTer Stranded Total RNA-Seq Kit v2 - Pico  
132 Input Mammalian (Takara Bio, #634413). The library preparation protocol started from 6  $\mu$ L  
133 eluate for the biofluid samples and 100 ng (or 10 ng) RNA for FFPE and MAQC. The  
134 recommended amount of input RNA for SMARTer Stranded Total RNA sequencing is only up  
135 to 10 ng while the capture method uses 100 ng. To make sure our analyses were not biased,  
136 we decided to use the total RNA-seq method with 100 ng RNA input as well but also included  
137 10 ng input samples. As shown in SFig 6 the results of 10 vs 100 ng RNA are similar. LncRNAs  
138 that are only detected using one of the input amounts are mostly low abundant lncRNAs that  
139 are just below the threshold. Compared to the manufacturer's protocol, the fragmentation  
140 step was set to 2 min at 94 °C, hereafter the option to start from high-quality or partially  
141 degraded RNA was used. During the final RNA seq library amplification, 16 PCR cycles were  
142 used for the samples derived from platelet depleted (blood) plasma, 12 PCR cycles were used  
143 for the other samples, and the cycles were followed by an extra 2 min at 68 °C before cooling  
144 them down to 4 °C. Library quality control was performed with the Fragment Analyzer high  
145 sense small fragment kit (Agilent Technologies, sizing range 50 bp-1000 bp). As Fragment  
146 Analyzer profiles showed the presence of multiple adapter dimers, the final AMPure Bead  
147 Purification step was repeated (17  $\mu$ l AMPure beads added to each sample - 20  $\mu$ l Tris Buffer  
148 was used to resuspend the beads – and elution volume of 18  $\mu$ l).

149 *Custom RNA capture library preparation*

150 Custom RNA capture-based libraries were prepared starting from 8.5  $\mu$ L eluate for biofluid  
151 samples and 100 ng RNA for FFPE and MAQCA/B using the TruSeq RNA Exome Library Prep  
152 Kit (Illumina, USA). Library preparation happened according to the manufacturer's protocol  
153 with some minor modifications. Fragmentation of RNA with the thermal cycler was set for 2  
154 min at 94 °C (instead of 8) and incubation to synthesize first strand cDNA for 30 min at 16 °C  
155 (instead of 60 min). After library validation with Fragment Analyzer (Agilent Technologies),  
156 the Twist Human Core Exome EF Multiplex protocol (Twist Bioscience, San Francisco, USA)  
157 was used starting with the pooling of amplified indexed libraries in sets of eight. One pool  
158 consisted of MAQCA/B and seminal plasma libraries (with the required 187.5 ng per sample),

159 the other pool was a low-input pool containing the FFPE and (blood) plasma libraries (with  
160 the available 20 ng per sample). Heated hybridization mix was added to the custom capture  
161 probes without cooling down to room temperature in order to prevent the probes from  
162 precipitating. After hybridization of probes with pools and binding to streptavidin beads, post  
163 capture PCR amplification was performed at 8 cycles for the high-input pool and 12 cycles for  
164 the low-input pool. After cleanup, the final libraries were validated with Fragment Analyzer  
165 (Agilent Technologies).

#### 166 *Sequencing*

167 Based on qPCR quantification with the KAPA Library Quantification Kit (Roche Diagnostics,  
168 #KK4854), samples were pooled and loaded on NextSeq 500 with a loading concentration of  
169 1.6 pM for the custom RNA capture libraries and 1.3 pM for the SMARTer Stranded Total RNA  
170 libraries. Paired end sequencing was performed (2 x 75 nucleotides). Custom RNA capture  
171 sequencing resulted in 168 million PE reads (median: 8.4 million PE reads/sample), SMARTer  
172 Stranded Total RNA sequencing resulted in 110 million PE reads (median: 10.5 million PE  
173 reads/sample). FASTQ data is currently being deposited in EGA.

#### 174 *Sequencing data quality control*

175 The SMARTer Stranded Total RNA seq libraries were trimmed using cutadapt (v.1.16) to  
176 remove 3 nucleotides of the 5' end of read 2 (Martin, 2011). Reads with a low a base calling  
177 accuracy (< 99% in at least 80% of the bases in both mates) were discarded. To enable a fair  
178 comparison, we started data-analysis from an equal number of reads by downsampling to the  
179 minimum available paired-end reads per sample type (rounded to half a million): 6.5 million  
180 for FFPE, 7.5 million for MAQCA/B, 6 million for seminal plasma, 3 million for platelet-  
181 depleted (blood) plasma. Downsampling was done with Seqtk (v1.3) (Li, 2021). Next, read  
182 duplicates were removed with Clumpify (BBMap v.38.26, standard settings) using the  
183 following specifications: paired-end mode, 2 substitutions allowed, kmersize of 31, and 20  
184 passes (Bushnell, 2021). For duplicate removal, only the first 60 nucleotides of both reads  
185 were considered to account for the sequencing quality drop at the end of the reads. Full-  
186 length read sequences were retrieved after duplicate removal for further quantification.

#### 187 *Quantification of Ensembl and LNCipedia genes*

188 Strand-specific transcript-level quantification of the deduplicated FASTQ files was performed  
189 with Kallisto (v.0.44.0) in -rf-stranded mode (Bray *et al.*, 2016). Quantification was performed  
190 with two references. The first one is a custom Ensembl v75 reference where lncRNAs are only

191 taken from LNCipedia 5.2 (high-confidence set) (Volders *et al.*, 2019; Yates *et al.*, 2020). This  
192 reference was used to design the custom probes. The second reference is only based on a  
193 more recent version of Ensembl v91.

194 Further processing was done with R (v.4.0.3) making use of tidyverse (v.1.3.0). A count  
195 threshold for filtering low abundant genes was set based on an analysis of single positive  
196 genes in technical replicates (Mestdagh *et al.*, 2014). Single positives are genes with a zero  
197 count value in one replicate and a non-zero value in the other one. After applying a threshold  
198 of 10 counts, at least 95% of the single positives are removed (SFig 3).

199

## 200 Results

201 In brief, 565,878 lncRNA capture probes of 120 nucleotides in length were designed against  
202 the high confidence set of LNCipedia v5.2 (Volders *et al.*, 2019) that comprises 107,039  
203 transcripts belonging to 49,372 lncRNA genes. This probe set targets 45,284 lncRNA genes or  
204 91.72% of the LNCipedia high confidence set. The median number of probes designed per  
205 lncRNA is 5 (SFig 1a), ranging from 1 up to 1675 probes for lnc-TBC1D22A-4 (with a length of  
206 152,544 bp). The selected probe designs have a median GC of 43.33%, a T<sub>m</sub> of 72.42 °C and  
207  $\Delta G$  of -2.8 (SFig 1b,c,d).

208 The custom lncRNA capture approach was applied to RNA from four different human sample  
209 types: high-quality RNA (artificial RNA mixture from human cell lines, MAQCA, and human  
210 brain reference RNA, MAQCB (Shi *et al.*, 2006)), formalin-fixed paraffin embedded colon  
211 tissue samples (FFPE), platelet-depleted blood plasma and seminal plasma. Each sample was  
212 also profiled with a total RNA-sequencing workflow representing the gold standard for  
213 quantification of both polyadenylated and non-polyadenylated lncRNAs.

214 We observed a clear enrichment of the lncRNA fraction with custom lncRNA capture  
215 compared to total RNA-seq when mapping reads to a LNCipedia transcriptome reference. Up  
216 to 75% of mapped reads in the custom capture method are derived from lncRNAs (Fig 1a),  
217 which is a 3.5-fold enrichment compared to total RNA-seq for FFPE, 4-fold for high quality  
218 MAQCA/B RNA and 8.5-fold for seminal plasma. This enrichment was also observed when  
219 aligning reads to a less comprehensive lncRNA reference (the Ensembl v91 reference),  
220 although the level of enrichment was lower (SFig 2a). In blood plasma, only a small fraction  
221 of reads aligned to lncRNAs for both the custom lncRNA capture and total RNA-seq method,



222 resulting in the detection of just a few hundred lncRNAs (data not shown). In FFPE, the  
223 fraction of reads mapping to ribosomal RNA was higher in total RNA-seq (38% and 52% for  
224 donor 1 and 2, respectively) compared to custom capture (10% and 20% for donor 1 and 2,  
225 respectively) (Fig 1a). In other sample types, the lower fraction of lncRNA reads in total RNA  
226 sequencing compared to custom capture sequencing is almost exclusively compensated by a  
227 higher fraction of protein coding RNA (mRNA) reads.

228 After downsampling to the same number of reads, we applied a minimal coverage of 10  
229 counts to select for lncRNAs that are reproducibly detected (SFig 3) and compared detection  
230 sensitivity between both methods. Although both methods were able to detect several  
231 thousands of lncRNAs, the custom capture method on average resulted in two times more  
232 uniquely detected lncRNAs compared to total RNA-seq (Fig 1b). The maximum number of  
233 detected lncRNAs with the custom capture approach was 8186 for FFPE, 11,238 for  
234 MAQCA/B, and 6910 for seminal plasma. As expected, the majority of lncRNAs detected in all  
235 total RNA-seq replicates were also detected in all custom capture replicates: 87%-91% of  
236 lncRNAs based on LNCipedia reference (Fig 1c); 83%-91% based on Ensembl reference (SFig  
237 2c). More importantly, custom capture enabled the detection of several thousands of  
238 additional lncRNAs (59%-61% of all lncRNAs reproducibly detected by custom capture were  
239 not detected by total RNA-seq), illustrating the sensitivity of this procedure (Fig 1c & SFig 2c).  
240 Expression abundance analysis revealed that these uniquely detected lncRNAs are generally  
241 less abundant compared to lncRNAs detected by both methods (Fig 1d & SFig 2d).

242 Next, we evaluated reproducibility based on absolute log<sub>2</sub> fold changes of lncRNA abundance  
243 between technical replicates (ideally, these fold changes are close to zero). As shown in Fig 2  
244 and SFig 4, we observed a higher fraction of lncRNAs with a log fold change close to zero in  
245 the custom capture approach compared to the total RNA-seq approach, indicating a better  
246 reproducibility for the custom capture approach. Only the total RNA-seq data of seminal  
247 plasma from donor 1 showed better reproducibility (SFig 4e), yet the custom approach in  
248 general still had lower fold changes between technical replicates (Kolmogorov-Smirnov test  
249 p-value < 0.001). Note that seminal plasma from donor 1 also resulted in a lower number of  
250 unique lncRNAs than that of donor 2 (Fig 1b).

251 We also compared transcript coverage of lncRNAs that were detected with both approaches  
252 by looking at their TPM distributions. In general, coverage was higher in the custom capture  
253 approach than in total RNA-seq (Fig 2 & SFig 4). Median TPM values for the custom capture

254 and total RNA-seq approach, respectively, were 8.2 and 2.0 TPM in FFPE, 9.7 and 2.5 TPM in  
255 MAQCA/B, and 16.1 and 2.3 TPM in seminal plasma. In terms of gene body coverage, both  
256 methods covered the entirety of the lncRNA body with an expected lower coverage towards  
257 the 5' and 3' ends. The custom capture sequencing, however, showed a more pronounced  
258 reduction in coverage towards the 3' end of the lncRNAs compared to total RNA-seq (SFig 5).  
259 Finally, we wanted to further assess the relevance of the custom capture approach for  
260 biological or clinical applications. We evaluated the abundance of previously described  
261 prostate-cancer related lncRNAs (Helsmoortel et al., 2018) in seminal plasma samples  
262 between both methods. As shown in Fig 3, coverage of detected lncRNAs is consistently  
263 higher with custom capture sequencing than with total RNA-seq. In total, 16 prostate-cancer  
264 related lncRNAs were detected above threshold in at least one sample. While none of those  
265 lncRNAs were exclusively detected by total RNA-seq, five lncRNAs (LINC01564, lnc-HNF1A-1,  
266 lnc-SPATA31A6-6, PCA3, and PCAT7) were detected by custom capture sequencing only. The  
267 custom capture counts of these lncRNAs ranged from 11 to 40 when taking the mean of both  
268 technical replicates of donor 2. Yet, these lncRNAs (except LINC01564) did not reach the  
269 detection threshold in custom capture sequencing samples of donor 1. For the 11 lncRNAs  
270 that were detected with both methods, custom capture sequencing resulted in 2 to 15 times  
271 more counts compared to total RNA-seq with an average fold change of 6. This increased  
272 sensitivity could greatly benefit biomarker research.

273 In summary, these findings demonstrate the added value of our custom lncRNA capture  
274 method for applications aimed at establishing a more complete lncRNA expression landscape.

275

## 276 Discussion

277 An extensive enrichment combined with a higher coverage of lncRNAs may further improve  
278 our understanding of lncRNA association to various conditions or phenotypes. Studies aiming  
279 to identify lncRNA biomarkers could equally benefit from these advantages. We have  
280 demonstrated a superior performance of custom lncRNA capture sequencing compared to  
281 classic total RNA-sequencing, across different sample types. Fewer reads are consumed by  
282 RNA biotypes other than lncRNAs, which results in a better lncRNA coverage. Interestingly,  
283 we also observed a better lncRNA detection reproducibility between technical replicates for

284 the custom capture compared to total RNA-seq (Fig 2). Deeper sequencing could event  
285 further improve the performance.

286 The custom capture method, however, did not outperform the total RNA-sequencing method  
287 in platelet-depleted blood plasma. In these samples, both methods only detected a few  
288 hundred lncRNAs. This observation is in line with the fact that the extracellular mRNA  
289 concentration in this sample type is low (Hulstaert *et al.*, 2020). Additionally, the blood plasma  
290 samples were not sequenced at high depth (3 million paired-end reads before duplicate  
291 removal), suggesting that results may improve when generating more reads.

292 For 10 to 25% of lncRNAs that were uniquely detected with total RNA-seq, no probes were  
293 present in the custom capture probe set because of a failure to satisfy probe design  
294 requirements. About half of the lncRNAs with at least one custom probe were still detected  
295 in some of the capture libraries but failed to reach the threshold in other replicates (and  
296 where therefore labeled as undetected in these libraries). While data was downsampled to  
297 the same read depth, increasing sequencing depth may solve this discrepancy. Some of the  
298 lncRNAs did not have probes complementary to the transcript regions that were detected  
299 with total RNA-seq. Incorporating additional probes against those regions could further  
300 improve performance, although this would require loosening probe design criteria, which  
301 may result in more non-specific hybridization and off-target capture. For the remaining  
302 lncRNAs, further optimization of the probe designs may be required to enable proper capture.  
303 Note that the custom capture library preparation is considerably more expensive than total  
304 RNA-sequencing. The price difference is mainly driven by the large custom probe set. Of note,  
305 probe cost could be substantially reduced when offered off-the-shelf or by transitioning from  
306 a discovery phase to a validation phase, including only those probes that target lncRNAs of  
307 interest. In this study, the stranded TruSeq RNA Exome Library Prep Kit was used for the  
308 custom capture approach, but other library prep methods would work too.

309 Taken together, we demonstrated that lncRNA capture sequencing is able to detect a more  
310 diverse repertoire of lncRNAs compared to standard total RNA sequencing, and increases  
311 coverage as well as reproducibility in both high-quality high input as well as fragmented  
312 and/or low input RNA samples.

313

## 314 Acknowledgements

315 This work was supported by the Fund for Scientific Research Flanders (1226821N and  
316 1S07416N to C.E.; 1133120N to E.H.; 11C1621N to A.M.) and the Special Research Fund (BOF)  
317 of Ghent University (BOF.DOC.2019.0047.01). This research is partly funded by “RNA-MAGIC”  
318 and “LNCCA” Concerted Research Actions of Ghent University (BOF19/GOA/008 and  
319 BOF16/GOA/023), by “Kom Op Tegen Kanker” (Stand Up To Cancer, the Flemish cancer  
320 society) and by the Foundation Against Cancer.

321 The authors wish to thank Kathleen Schoofs for preparing platelet-depleted plasma from  
322 blood samples and Kimberly Verniers for providing purified RNA of FFPE samples as well as  
323 her input on the custom lncRNA capture protocol.

324 We are very grateful to Gary Schroth, Scott Kuersten and Stephen Gross (Illumina) for  
325 providing a prototype set of lncRNA probes to evaluate the custom hybrid capture procedure.

326

## 327 Conflict of interest

328 The authors declare no conflicts of interest.

329

## 330 References

331 Bray,N.L. *et al.* (2016) Near-optimal probabilistic RNA-seq quantification. *Nat. Biotechnol.*, **34**,  
332 525–527.

333 Bushnell,B. (2021) BBMap. *SourceForge*.

334 Cao,M. *et al.* (2019) Genome-wide methods for investigating long noncoding RNAs. *Biomed.*  
335 *Pharmacother.*, **111**, 395–401.

336 Clark,M.B. *et al.* (2015) Quantitative gene profiling of long noncoding RNAs with targeted RNA  
337 sequencing. *Nat. Methods*, **12**, 339–342.

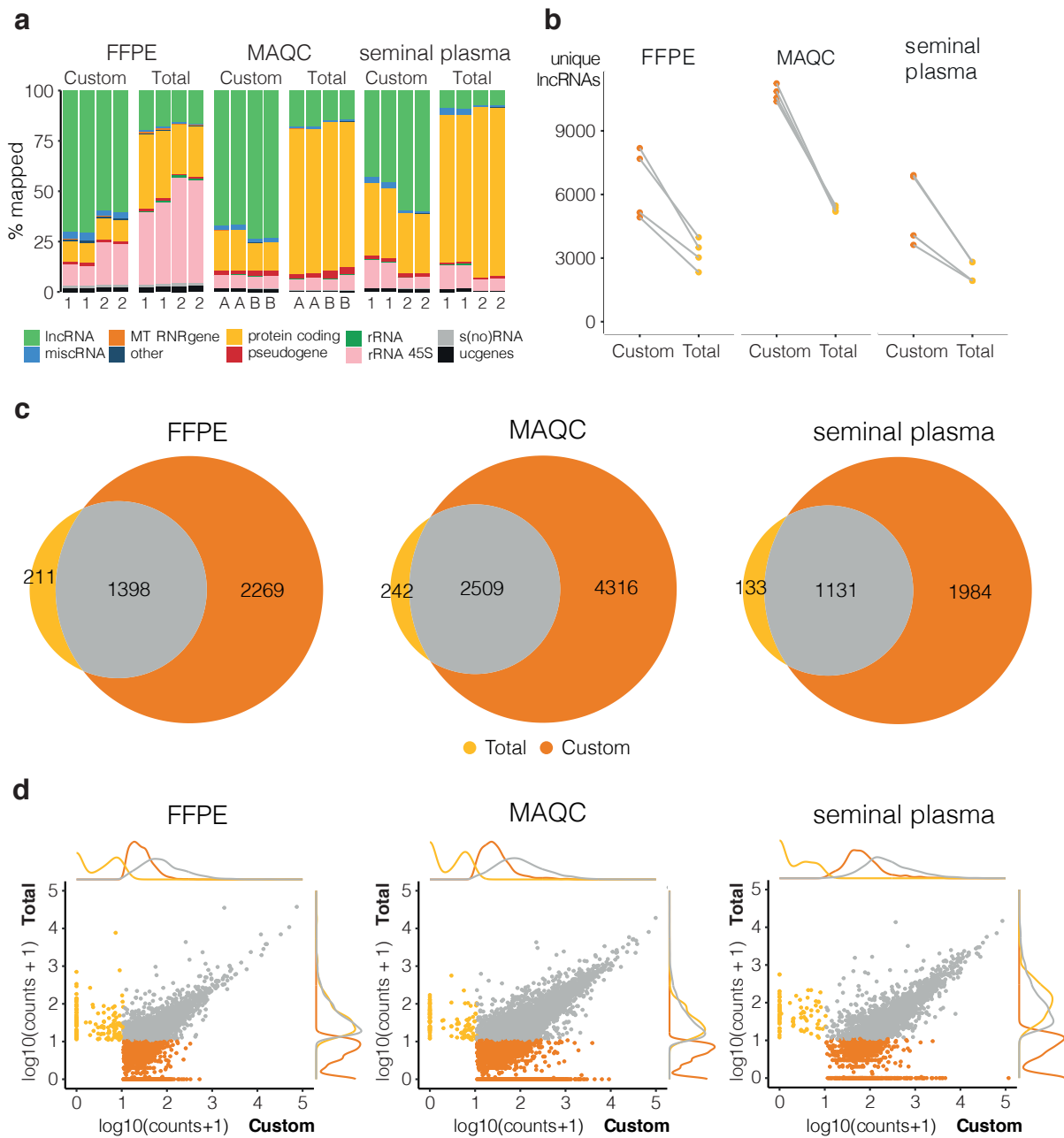
338 Djebali,S. *et al.* (2012) Landscape of transcription in human cells. *Nature*, **489**, 101–108.

339 Helmoortel,H. *et al.* (2018) Detecting long non-coding RNA biomarkers in prostate cancer  
340 liquid biopsies: Hype or hope? *Non-Coding RNA Res.*, **3**, 64–74.

341 Hulstaert,E. *et al.* (2020) Charting Extracellular Transcriptomes in The Human Biofluid RNA  
342 Atlas. *Cell Rep.*, **33**, 108552.

- 343 Iyer,M.K. *et al.* (2015) The landscape of long noncoding RNAs in the human transcriptome.  
344 *Nat. Genet.*, **47**, 199–208.
- 345 Lagarde,J. *et al.* (2017) High-throughput annotation of full-length long noncoding RNAs with  
346 Capture Long-Read Sequencing. *Nat. Genet.*, **49**, 1731–1740.
- 347 Li,H. (2021) lh3/seqtk.
- 348 Lorenzi,L. *et al.* (2019) The RNA Atlas, a single nucleotide resolution map of the human  
349 transcriptome. *bioRxiv*, 807529.
- 350 Martin,M. (2011) Cutadapt removes adapter sequences from high-throughput sequencing  
351 reads. *EMBnet.journal*, **17**, 10–12.
- 352 Mercer,T.R. *et al.* (2009) Long non-coding RNAs: insights into functions. *Nat. Rev. Genet.*, **10**,  
353 155–159.
- 354 Mercer,T.R. *et al.* (2014) Targeted sequencing for gene discovery and quantification using  
355 RNA CaptureSeq. *Nat. Protoc.*, **9**, 989–1009.
- 356 Mestdagh,P. *et al.* (2014) Evaluation of quantitative miRNA expression platforms in the  
357 microRNA quality control (miRQC) study. *Nat. Methods*, **11**, 809–815.
- 358 Robinson,E.K. *et al.* (2020) The how and why of lncRNA function: An innate immune  
359 perspective. *Biochim. Biophys. Acta Gene Regul. Mech.*, **1863**, 194419.
- 360 Shi,L. *et al.* (2006) The MicroArray Quality Control (MAQC) project shows inter- and  
361 intraplatform reproducibility of gene expression measurements. *Nat. Biotechnol.*, **24**,  
362 1151–1161.
- 363 Turner,A.W. *et al.* (2019) Multi-Omics Approaches to Study Long Non-coding RNA Function in  
364 Atherosclerosis. *Front. Cardiovasc. Med.*, **6**.
- 365 Volders,P.-J. *et al.* (2019) LNCipedia 5: towards a reference set of human long non-coding  
366 RNAs. *Nucleic Acids Res.*, **47**, D135–D139.
- 367 Yates,A.D. *et al.* (2020) Ensembl 2020. *Nucleic Acids Res.*, **48**, D682–D688.
- 368

369 Figures

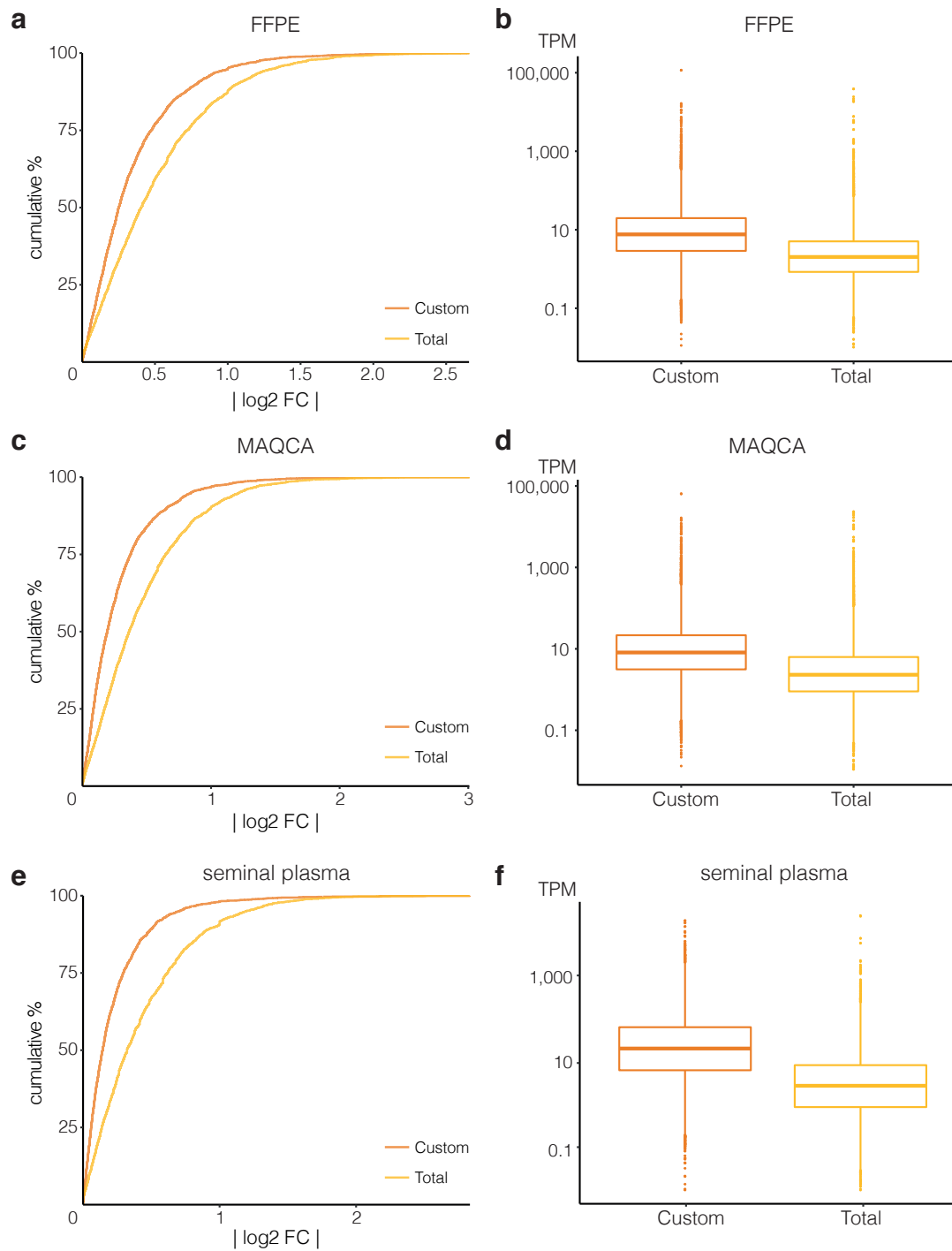


370

371 **Fig 1: Custom capture sequencing (Custom) is able to detect more lncRNAs than total RNA-**  
 372 **sequencing (Total).** Quantification based on combined reference of Ensembl and LNCipedia.

373 a: RNA biotype distribution plot of mapped reads where 1 and 2 indicate the two different  
 374 donors and A and B refer to MAQCA and MAQCB, respectively (lncRNAs: high-confidence  
 375 lncRNAs based on LNCipedia 5.2; miscRNA: miscellaneous RNA, non-coding RNA that cannot  
 376 be classified; MT RNR gene: mitochondrially encoded ribosomal RNAs; protein coding: protein  
 377 coding RNA transcripts; pseudogene; rRNA (45S): (45S) ribosomal RNA; s(no)RNA: small  
 378 nuclear/nucleolar RNA; ucgenes: unannotated cancer genes; other: T cell receptor genes,

379 Immunoglobulin genes, TEC (To be Experimentally Confirmed) - regions with EST clusters that  
380 have polyA features that could indicate the presence of protein coding genes, vaultRNA -  
381 short non coding RNA genes that form part of the vault ribonucleoprotein complex;  
382 microRNAs; ribozymes); b: number of unique lncRNAs with at least 10 counts (filter  
383 threshold), data points from same donor or MAQC type are linked (grey lines); c: overlap  
384 between lncRNAs that are detected above threshold in all replicates of a certain library prep  
385 method, plots made with eulerr package (v6.1.0) in R; d: correlation and density plots of  
386 overlapping (grey) and specific lncRNAs for custom capture (orange) and total RNA-  
387 sequencing (yellow); lncRNAs below count threshold in both methods were left out.



388

389 **Fig 2: Custom capture seq (Custom) has a higher lncRNA count reproducibility and coverage**

390 **than total RNA-seq (Total).** Cumulative distributions of absolute log<sub>2</sub> fold changes (log<sub>2</sub> FC)

391 between lncRNA counts in the two technical replicates are shown for (a) FFPE from donor 1,

392 (c) MAQCA, and (e) seminal plasma from donor 2. Kolmogorov–Smirnov tests each time

393 showed significant difference in distributions between Total and Custom (p-value < 0.001).

394 Boxplot of corresponding transcripts per million (TPM) values of these lncRNAs are shown in

395 (b) for FFPE, (d) for MAQCA, and (f) for seminal plasma.



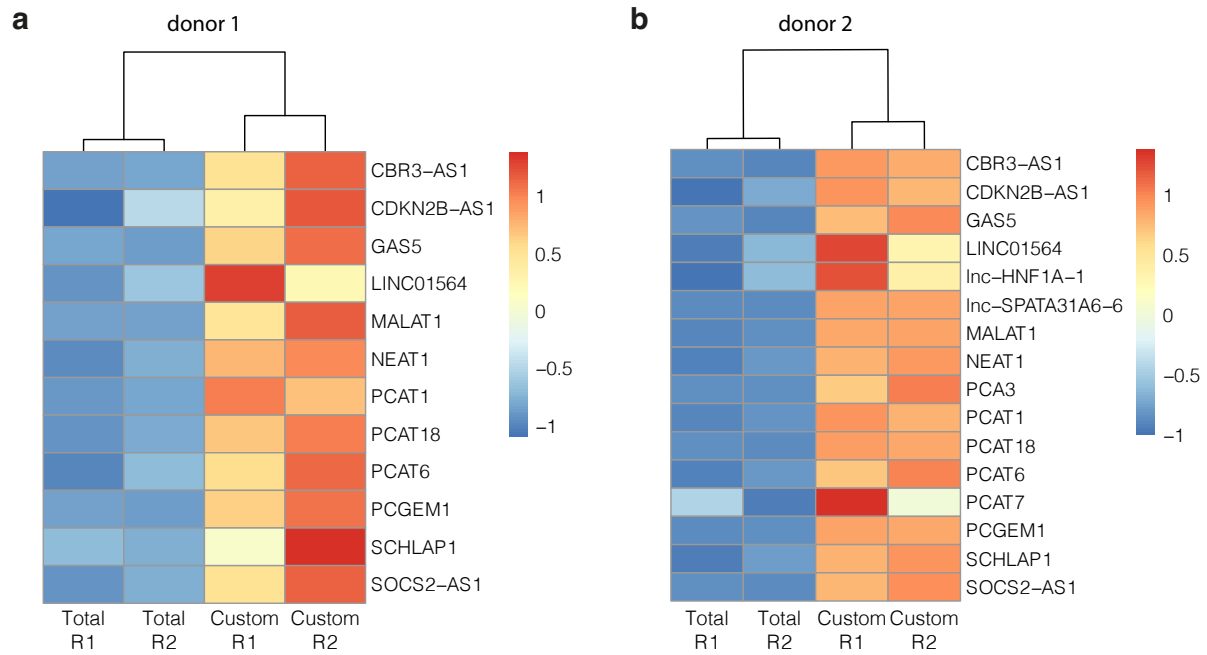
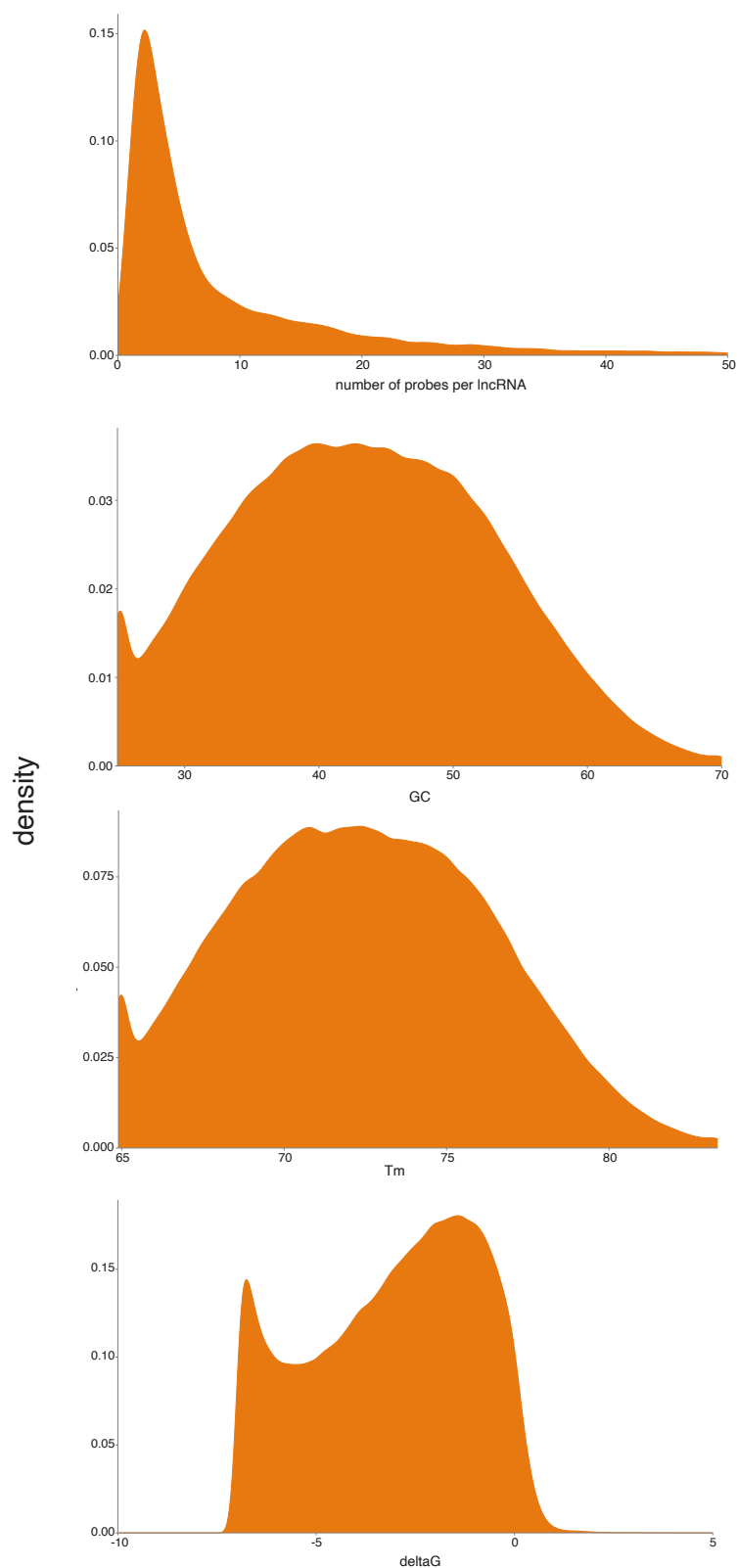


**Fig 3: Higher coverage for prostate-cancer related lncRNAs with custom capture (Custom) than total RNA-sequencing (Total).** Heatmaps based on z-score transformed lncRNA counts of seminal plasma samples from donor 1 (a) and donor 2 (b), respectively. Per donor, only lncRNAs detected above count threshold (10 counts) in at least one replicate were considered. A higher z-score (orange/red) indicates relatively more coverage. Complete clustering of samples based on Euclidean distance. R1: technical replicate 1; R2: technical replicate 2.

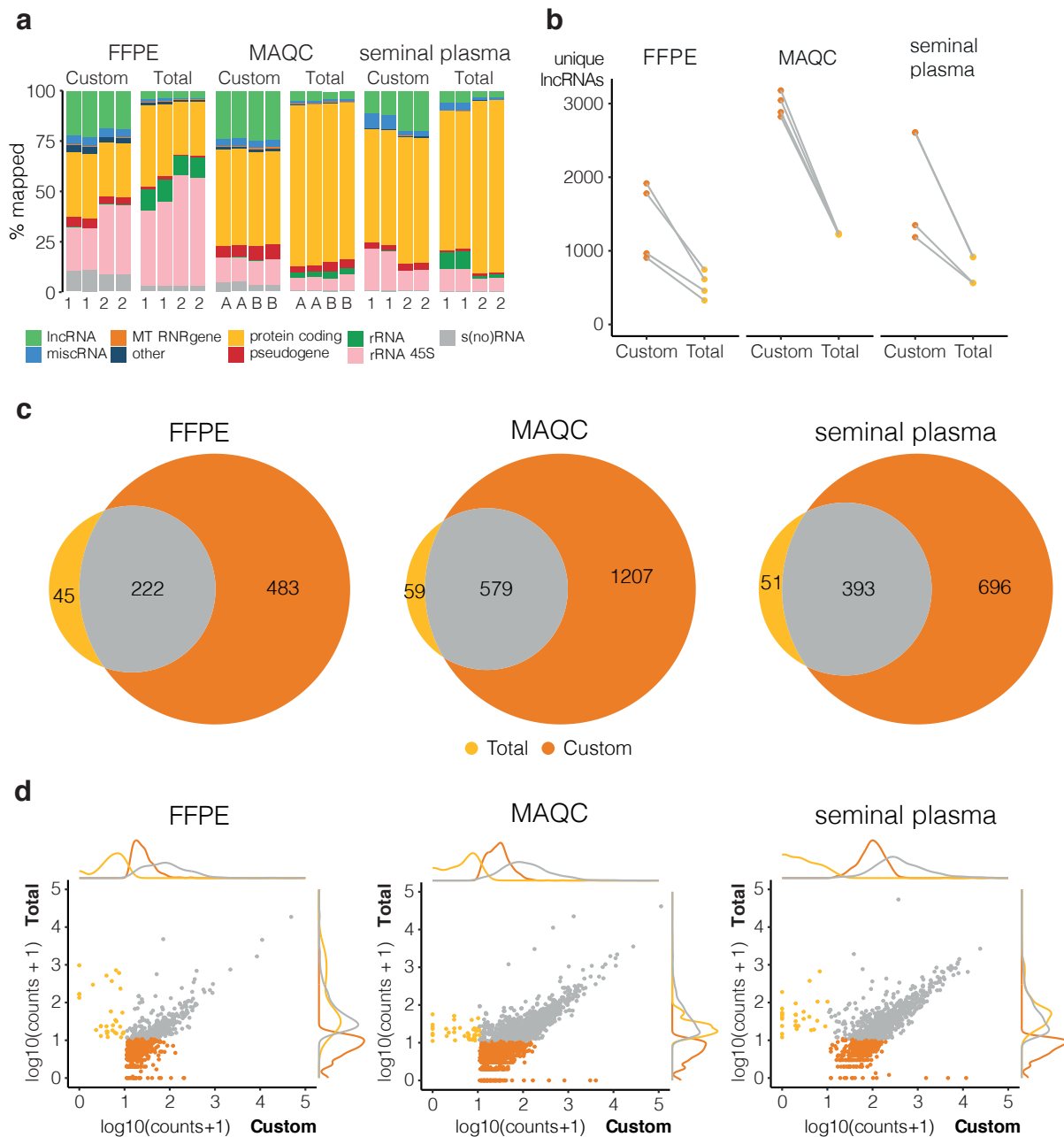
## 405 Supplemental Figures



406

407 **SFig 1: Distributions of number of probes per gene, GC%, melting temperature and  $\Delta G$  of**

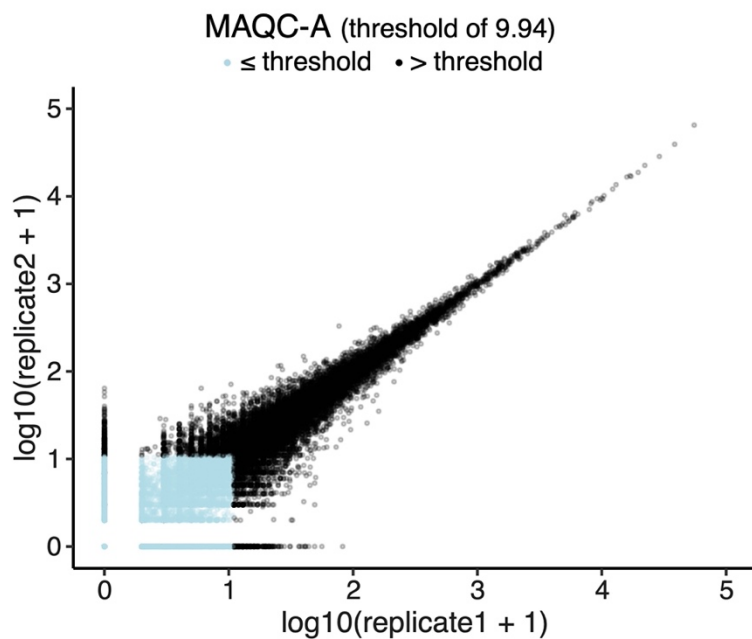
408 **the selected probes.**



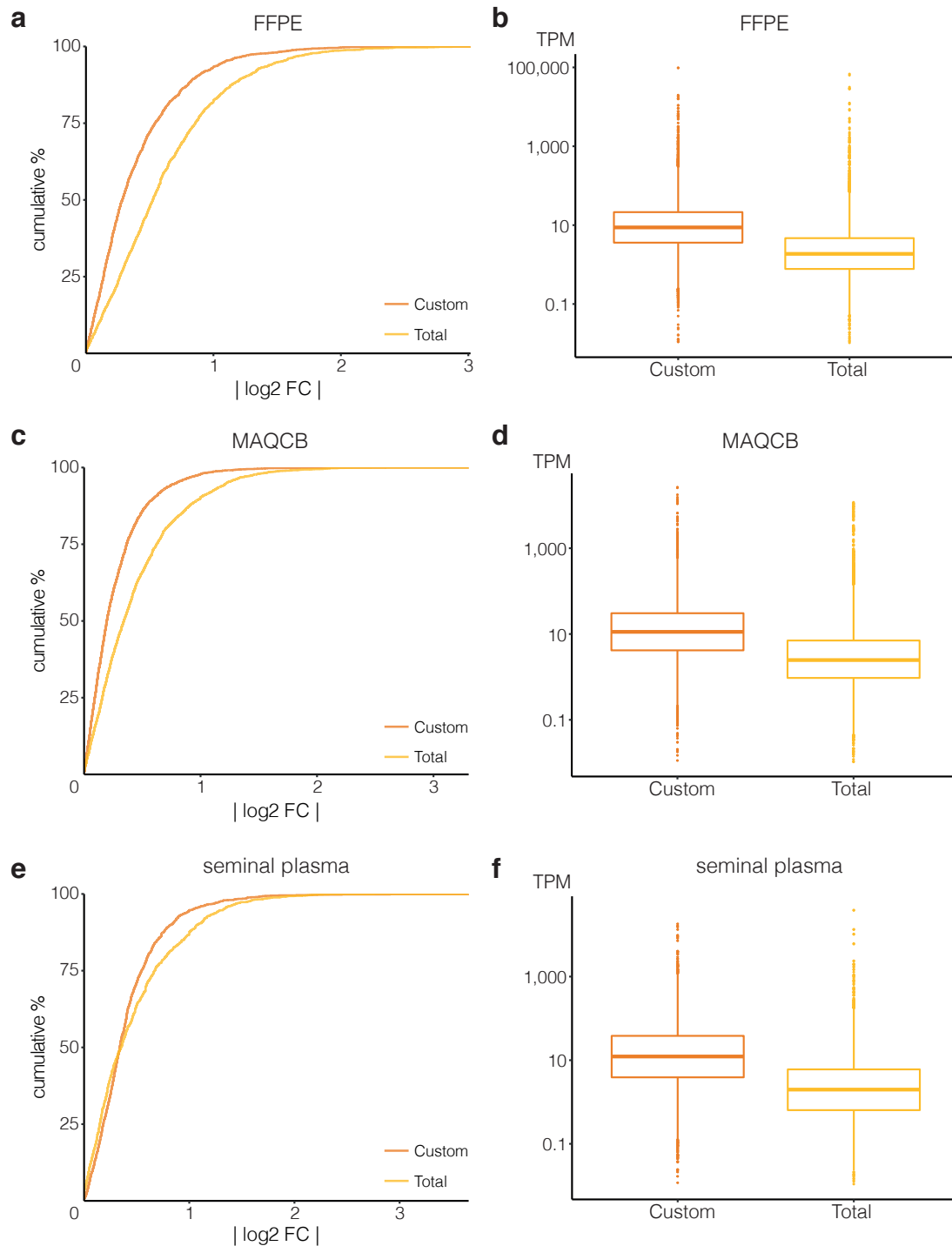
409

410 **SFig 2: Custom capture sequencing (Custom) is able to detect more lncRNAs than**  
 411 **total RNA-sequencing (Total).** Quantification based on Ensembl v91 reference. a: RNA biotype  
 412 distribution plot of mapped reads where 1 and 2 indicate the two different donors and A and  
 413 B refer to MAQCA and MAQCB, respectively (lncRNAs: Ensembl lncRNAs; miscRNA:  
 414 miscellaneous RNA, non-coding RNA that cannot be classified; MT RNR gene: mitochondrially  
 415 encoded ribosomal RNAs; protein coding: protein coding RNA transcripts; pseudogene; rRNA  
 416 (45S): (45S) ribosomal RNA; s(no)RNA: small nuclear/nucleolar RNA; ucgenes: unannotated  
 417 cancer genes; other: T cell receptor genes, Immunoglobulin genes, TEC (To be Experimentally  
 418 Confirmed) - regions with EST clusters that have polyA features that could indicate the

419 presence of protein coding genes, vaultRNA - short non coding RNA genes that form part of  
420 the vault ribonucleoprotein complex; microRNAs; ribozymes); b: number of unique lncRNAs  
421 with at least 10 counts (filter threshold), data points from same donor are linked (grey lines);  
422 c: overlap between lncRNAs that are detected above threshold in all replicates of a certain  
423 library prep method, plots made with eulerr package (v6.1.0) in R; d: correlation and density  
424 plots of overlapping (grey) and specific lncRNAs for custom capture (orange) and total RNA-  
425 sequencing (yellow); lncRNAs below count threshold in both methods were left out.  
426



427  
428 **SFig 3: Reproducibility threshold is determined based on elimination of at least 95% of**  
429 **single positives between technical (library preparation) replicates.** Single positives are  
430 detected (at least 1 count) in one replicate and not detected in the other replicate. Here,  
431 example of replicate correlation of MAQCA with total RNA sequencing is shown. Count  
432 threshold that filters out 95% of single positives is 9.94 (kallisto quantification leads to decimal  
433 counts). Data points that will be filtered with this threshold are in blue. Slope of linear model  
434 is 0.969, pearson correlation is 0.999.



435

436 **SFig 4: Custom capture seq (Custom) has a higher lncRNA count reproducibility and**

437 **coverage than SMARTer Stranded Total RNA seq (Total).** Cumulative distribution of absolute

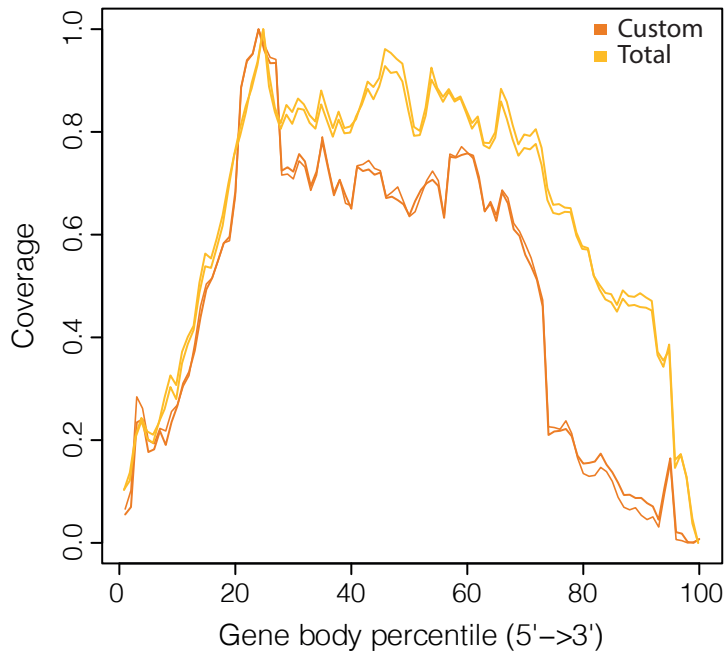
438 log<sub>2</sub> fold changes between lncRNA counts in the two technical replicates are shown for (a)

439 FFPE from donor 2, (c) MAQCB, and (e) seminal plasma from donor 1. Kolmogorov–Smirnov

440 tests each time showed significant difference in distributions between Total and Custom (p-

441 value < 0.001). Boxplot of corresponding transcripts per million (TPM) values of these lncRNAs

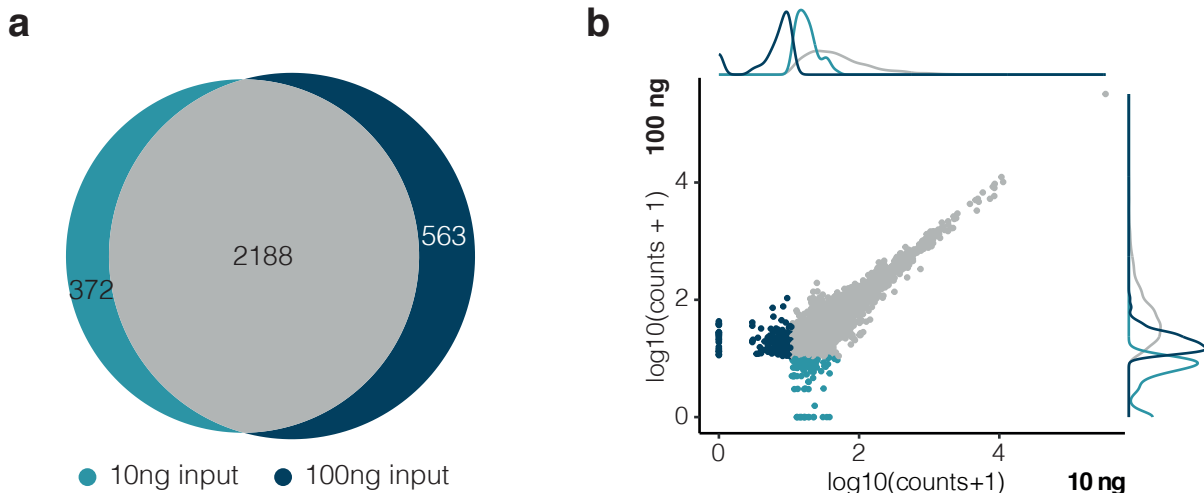
442 are shown in (b) for FFPE, (d) for MAQCB, and (f) for seminal plasma.



443

444 **SFig 5: Distribution of gene body coverage shows quite stable coverage for majority of gene**  
445 **(lncRNA) body but drops towards the 5' and 3' ends.** Distribution shown for both technical  
446 replicates of MAQCA. Custom: custom capture sequencing; Total: SMARTer Stranded Total  
447 RNA sequencing.

448



449

450 **SFig 6: Impact of 10 vs 100 ng RNA input on SMARTer Stranded Total RNA sequencing results**  
451 **is limited.** a: overlap between lncRNAs detected (> 10 counts) in MAQC with 10 vs 100 ng RNA  
452 input for library preparation; b: corresponding count correlation and density plot (counts  
453 shown for one technical replicate of MAQCA).